Atmos. Chem. Phys., 25, 17009–17025, 2025 https://doi.org/10.5194/acp-25-17009-2025 © Author(s) 2025. This work is distributed under the Creative Commons Attribution 4.0 License.





# Uncertainties in fertilizer-induced emissions of soil nitrogen oxide and the associated impacts on ground-level ozone and methane

Cheng Gong<sup>1</sup>, Yan Wang<sup>2</sup>, Hanqin Tian<sup>3,4</sup>, Sian Kou-Giesbrecht<sup>5</sup>, Nicolas Vuichard<sup>6</sup>, and Sönke Zaehle<sup>1</sup>

<sup>1</sup>Max Planck Institute for Biogeochemistry, Jena, 07745, Germany
 <sup>2</sup>State Key Laboratory for Development and Utilization of Forest Food Resources, College of Environment and Resources, College of Carbon Neutrality, Zhejiang A&F University, Hangzhou, 311300, China
 <sup>3</sup>Center for Earth System Science and Global Sustainability, Schiller Institute for Integrated Science and Society, Boston College, Chestnut Hill, MA, USA

<sup>4</sup>Department of Earth and Environmental Sciences, Boston College, Chestnut Hill, MA, USA
<sup>5</sup>School of Resource and Environmental Management, Simon Fraser University, Burnaby, BC, Canada
<sup>6</sup>Laboratoire des Sciences du Climat et de l'Environnement, LSCE-IPSL (CEA-CNRS-UVSQ),
Université Paris-Saclay, Gif-sur-Yvette, France

**Correspondence:** Cheng Gong (cgong@bgc-jena.mpg.de)

Received: 25 March 2025 – Discussion started: 12 May 2025 Revised: 20 August 2025 – Accepted: 30 October 2025 – Published: 27 November 2025

**Abstract.** Natural and agricultural soils are important sources of nitrogen oxides (NO<sub>x</sub>), accounting for about 10%-20% of the global NO<sub>x</sub> emissions. The increased application of nitrogen (N) fertilizer in agriculture has strongly enhanced the N availability of soils in the last several decades, leading to higher soil  $NO_x$  emissions. However, the magnitude of the N fertilizer-induced soil NO<sub>x</sub> emissions remains poorly constrained due to limited field observations, resulting in divergent estimates. Here we integrate the results from meta-analyses of field manipulation experiments, emission inventories, atmospheric chemistry modelling and terrestrial biosphere modelling to investigate these uncertainties and the associated impacts on ground-level ozone and methane. The estimated present-day global soil NO<sub>x</sub> emissions induced by N fertilizer application vary substantially (0.84– 2.2 Tg N yr<sup>-1</sup>) among different approaches with different spatial patterns. Simulations with the 3-D global chemical transport model GEOS-Chem demonstrate that N fertilization enhances global surface ozone concentrations during summertime in agricultural hotspots, such as North America, western Europe and eastern and southern Asia by 0.1 to 3.3 ppbv (0.2 %–7.0 %). Our results show that such spreads in soil  $NO_x$  emissions also affect atmospheric methane concentrations, reducing the global mean by 6.7 (0.4%) ppbv to 16.6 (0.9%) ppbv as an indirect consequence of enhanced N fertilizer application. These results highlight the urgent need to improve the predictive understanding of soil NO<sub>x</sub> emission responses to fertilizer N inputs and its representation in atmospheric chemistry modelling.

#### 1 Introduction

Nitrogen oxides ( $NO_x = NO + NO_2$ ), as one of the most important reactive atmospheric components, strongly affect the atmospheric oxidation capacity and further influence air quality (Gong et al., 2020; Zhai et al., 2021; Goldberg et al., 2022; Zhao et al., 2023), radiative forcing (Erisman et al., 2011; Pinder et al., 2012; Gong et al., 2024), as well as carbon (C) storage in terrestrial and marine ecosystems (Fowler et al., 2013; Fleischer et al., 2019; Rubin et al., 2023). The major source of present-day atmospheric  $NO_x$  is fossil fuel combustion (Martin et al., 2003; Hoesly et al., 2018), but several non-fossil-fuel sources, including emissions from soils, lightning and wildfire (Zhang et al., 2003), contribute around 30 % of the global total  $NO_x$  emissions (Delmas et al., 1997; Weng et al., 2020). However, these non-fossil-fuel sources have been widely regarded as "natural" sources, where the perturbation by anthropogenic activities as well as the associated potentially significant effects on the N cycle are often overlooked. Meanwhile, strict clean-air actions have been applied in many countries in the past decades to sharply reduce the fossil-fuel sources of  $NO_x$  (Jiang et al., 2022). As a result, non-fossil sources of  $NO_x$  will be increasingly important for future clean air policies.

One of the most important non-fossil-fuel anthropogenic sources of  $NO_x$  is through agricultural activities, which have been estimated to enhance soil  $NO_x$  emissions by around 5 %–30 % (Wang et al., 2022; Gong et al., 2024). To assess the soil  $NO_x$  emissions induced by N fertilizer application (hereafter, SNO<sub>x</sub>-Fer), the most straightforward and widelyused method is applying the emission factor (EF), which indicates the proportion of N from fertilizer application emitted as  $NO_x$ . The Intergovernmental Panel on Climate Change (IPCC) methodology recommended a constant EF value of 1.1 % with an uncertainty range of 0.06 % to 2.18 % (Buendia et al., 2019). Other studies recommend slightly smaller uncertainty ranges (0.47 % to 1.61 %) based on different metaanalysis datasets (Stehfest and Bouwman, 2006; Liu et al., 2017; Skiba et al., 2021; Wang et al., 2022). This large uncertainty range results from the dependency of the response of soil NO<sub>x</sub> emissions on intricate soil biogeochemical processes, and it varies with crop types, soil texture, fertilizer types and application rate (Wang et al., 2022). To date, limited field experiments are available to constrain this uncertainty range.

Some studies have suggested using non-linear EF to take account of the observations that the EFs of soil reactive nitrogen gases tend to increase with increasing fertilizer application (Shcherbak et al., 2014; Jiang et al., 2017). Such an approach assumes that plants and soil microbes should have priority in accessing soil available N for their metabolic activities, while the excessive inorganic N can be used by nitrifiers and denitrifiers and loses as the gas form. Such a non-linear EF approach is more ecologically reasonable but there remain large uncertainties in assessing soil  $NO_x$  due

to the limited available field data. For example, Wang et al. (2024) examined the non-linear EF of soil  $NO_x$  based on a global meta-analysis and found a much lower EF (around 0 %–0.7 %) than the IPCC-recommended linear EF (1.1 %) within the range of normal agricultural crop N fertilizer loading (around 0–600 kg N ha<sup>-1</sup> yr<sup>-1</sup>).

In many of the atmospheric chemical transport models (CTMs), SNO<sub>x</sub>-Fer is represented by the agriculture sector of NO<sub>x</sub> emission from an anthropogenic emission inventory (e.g. Emissions Database for Global Atmospheric Research (EDGAR) or Community Emissions Data System (CEDS)), which in general apply the linear EF method to estimate the agricultural  $NO_x$  emissions (Hoesly et al., 2018; Janssens-Maenhout et al., 2019; Hutchings et al., 2023) with the caveats described above. Furthermore, some advanced CTMs, e.g. the GEOS-Chem model, parametrize soil NO<sub>x</sub> emissions as a function of N availability as well as soil temperature and soil moisture (Steinkamp and Lawrence, 2011; Hudman et al., 2012). The currently widely used soil NO<sub>x</sub> scheme, known as the Berkeley-Dalhousie Soil NO<sub>x</sub> Parameterization (BDSNP), could dynamically simulate the spatiotemporal variations of soil  $NO_x$  emissions, however, the responses of soil  $NO_x$  to N fertilizer application are not fully examined (See the detailed parameterization in Sect. 2).

Recently, another approach to modelling  $SNO_x$ -Fer has emerged with the development of global, process-based terrestrial biosphere models (TBMs) with fully-coupled C and N cycles (Zaehle and Friend, 2010; Tian et al., 2019). Driven by data of N inputs (synthetic N fertilizer, N manure application and N deposition), CO<sub>2</sub> concentrations and climate, these TBMs could simulate the coupled cycles of C and N in the terrestrial biosphere, mimic the competition on the available N between plants and microbes and calculate the rates of nitrification and denitrification (Zaehle and Dalmonech, 2011), which are the two microbial processes that determine the rates of soil  $NO_x$  emissions. Even though TBMs provide a more ecologically-mechanistic description of the terrestrial N cycles, large uncertainties remain among different TBMs due to the varying parameterization and modelling schemes in biome N use strategies, mineralization of organic N, nitrification and denitrification processes (Kou-Giesbrecht et al., 2023), which lead to varied responses of soil  $NO_x$  to the increased N fertilizer inputs (Gong et al., 2024).

In this study, we attempt to comprehensively quantify the uncertainties in current  $SNO_x$ -Fer estimates by integrating results from meta-analyses, emission inventories, as well as CTMs and TBMs. We use this understanding to assess the associated effects of  $SNO_x$ -Fer uncertainties on global  $O_3$  and  $CH_4$  concentrations. Section 2 will introduce the N synthetic fertilizer and manure input data and the approaches used to estimate  $SNO_x$ -Fer. Section 3 will introduce the CTM used in this study and the configuration of sensitivity experiments. Section 4 will first show the variations of  $SNO_x$ -Fer among different approaches as well as the seasonal dynamics, and then analyze the associated uncertainties in global  $O_3$  and

CH<sub>4</sub> simulations. Finally, the conclusion and discussions of this study will be given in Sect. 5.

#### 2 Data and Methods

## 2.1 Linear and Non-linear EFs and the global fertilizer N dataset

We first implement the most traditional method with a constant EF value to estimate the effects of N fertilizer application on soil  $NO_x$  emissions, where the value of 1.1 % (1.1 % of N in the fertilizer will be emitted as  $NO_x$ ; named EF<sub>linear</sub> hereafter) based on the most up-to-date IPCC methodology is adopted (Buendia et al., 2019). Furthermore, based on the latest meta-analysis dataset developed by Wang et al. (2024), a non-linear EF method (EF<sub>non-linear</sub>) to describe the variations of soil  $NO_x$  emissions with different N fertilizer loadings is also applied:

$$EF_{non-linear} = (0.22 + 0.008 \times Fertilizer_{N})$$
 (1)

where the  $EF_{non-linear}$  (%) is the non-linear EF and  $Fertilizer_N$  is the loading of fertilizer N application (kg N ha<sup>-1</sup>). The detailed derivation of this formula is presented in Wang et al. (2024), which follows a comparable method as presented by Shcherbak et al. (2014).

We used the dataset of History of anthropogenic Nitrogen inputs (HaNi) (Tian et al., 2022) for the global rate of synthetic fertilizer and manure application, in order to estimate SNO<sub>x</sub>-Fer with both the linear and non-linear EF methods. The HaNi dataset includes grid-level annual loadings of (1) NH<sub>4</sub><sup>+</sup>-N synthetic fertilizer applied to cropland, (2) NO<sub>3</sub>-N synthetic fertilizer applied to cropland, (3) NH<sub>4</sub><sup>+</sup>-N synthetic fertilizer applied to pasture, (4) NO<sub>3</sub><sup>-</sup>-N synthetic fertilizer applied to pasture, (5) manure NH<sub>4</sub><sup>+</sup>-N application on cropland, (6) manure NO<sub>3</sub><sup>-</sup>-N application on pasture, (7) manure NH<sub>4</sub><sup>+</sup>-N deposition on pasture, and (8) manure NO<sub>3</sub><sup>-</sup>-N deposition on rangeland. We use a global map of land use class distribution (Hurtt et al., 2020) (Fig. S1 in the Supplement) to convert the unit of N loading in HaNi from gNgrid<sup>-1</sup> to kgN (hapasture)<sup>-1</sup>,  $kg N (ha rangeland)^{-1} or kg N (ha cropland^{-1}).$  The annual N inputs from the HaNi dataset, which are summed by all N forms of synthetic fertilizer and manure, are evenly applied in the months of the growing season, while the rates of N inputs are set as zero during the non-growing season. We define the growing season as monthly-mean 2 m temperature greater than 5 °C (based on the MERRA2 reanalyzed dataset, see below Sect. 3) and the grid-level monthly-mean leaf area index (LAI) larger than 0.5 (based on the MODIS remote sensing dataset post-processed by Yuan et al. (2011) and updated for the use of GEOS-Chem, http://geoschemdata.wustl.edu/ExtData/HEMCO/Yuan XLAI/v2021-06/, last access: 24 November 2025). Finally, the rates of synthetic fertilizer and manure N inputs in units utilized to estimate global  $SNO_x$ -Fer with both the linear and non-linear EF approaches (Fig. S2).

#### 2.2 The emissions inventory CEDS

We use the CEDS (Hoesly et al., 2018) for assessing the fertilizer-induced soil  $NO_x$  emissions in the emission inventories. CEDS is one of the most state-of-the-art emission inventories that comprehensively assesses the sources of dominant air pollutants from the pre-industrial period to the present day, which has been used as the standard emission inventory to drive CMIP6 models. The agricultural  $NO_x$  emission in CEDS is fromEDGAR 4.3.1 (https://edgar.jrc.ec. europa.eu/, last access: 24 November 2025), where the old IPCC methodology (Eggleston et al., 2006) is used with a constant EF value of 0.7 % (0.7 % of N in the fertilizer will be emitted as  $NO_x$ ) (Janssens-Maenhout et al., 2019).

## 2.3 The BDSNP scheme

The BDSNP scheme in CTMs was firstly developed by Yienger and Levy (1995), and then updated by Hudman et al. (2012). The emission of soil  $NO_x$  ( $S_{nox}$ ) is described as:

$$S_{\text{nox}} = (A_{\text{w,biome}} + N_{\text{avail}} \times \overline{E}) \times f(T) \times g(\theta) \times P(l_{\text{dry}})$$
 (2)

where f(T),  $g(\theta)$  and  $P(l_{\rm dry})$  indicate the effects of temperature, soil moisture and rain pulsing.  $A_{\rm w,biome}$  is the wet biome-dependent emission (the baseline emission) from Steinkamp and Lawrence (2011).  $N_{\rm avail}$  is the soil available N mass in the top 10 cm (ng N m<sup>-2</sup>), which is calculated by:

$$N_{\text{avail}}(t) = N_{\text{avail}}(0)e^{-\frac{t}{\tau}} + \text{Fertilizer}_{N} \times \tau \times (1 - e^{-\frac{t}{\tau}})$$
 (3)

where the initial soil available N mass  $N_{\text{avail}}(0)$  is prescribed. Fertilizer<sub>N</sub> is the rate of fertilizer N application, which is set to zero outside the growing season.  $\tau$  indicates the decay rate and is chosen as 4 months based on the measurements within the top 10 cm of soil (Matson et al., 1998; Cheng et al., 2004; Russell et al., 2011). However, it should be noted that the magnitude of global SNO<sub>x</sub>-Fer (i.e. the  $N_{\text{avail}} \times \overline{E}$ ) is scaled by the factor  $\overline{E}$  in Eq. (2) to meet  $1.8 \,\mathrm{Tg}\,\mathrm{N}\,\mathrm{yr}^{-1}$ before the canopy reduction, which is the value obtained in a previous meta-analysis study based on the fertilizer N input dataset in the 2000s (Stehfest and Bouwman, 2006). As a result, the default BDSNP scheme in GEOS-Chem actually fails to capture the year-to-year variations of soil  $NO_x$  emissions with the changing soil N availability. However, as the BDSNP scheme is still widely used by the community of atmospheric chemistry modelling (e.g. Lu et al., 2021; Wang et al., 2022; Huber et al., 2023), here we add another sensitivity experiment by scaling the  $N_{\text{avail}}$  in Eq. (3) following the interannual variations of the HaNi fertilizer loadings:

$$N_{\rm avail}(i,j,yr) = N_{\rm avail}(i,j,2000) \times \frac{\rm Fertilizer_{\rm HaNi}(i,j,yr)}{\rm Fertilizer_{\rm HaNi}(i,j,2000)} \quad (4)$$

of kg N (ha pasture/rangeland/cropland) $^{-1}$  month $^{-1}$ 

where Fertilizer $_{\text{HaNi}}(ijyr)$  represents the total N fertilizer loadings in the HaNi dataset at the grid of i latitude and j longitude in the yr year. With this modification, we could further examine how  $\text{SNO}_x$ -Fer responds to the N fertilizer enhancement in the GEOS-Chem BDSNP scheme.

#### 2.4 The TBM ensemble

Simulated soil  $NO_x$  emissions were provided by three TBMs (CLASSIC, OCN and ORCHIDEE) with fully-coupled C and N cycles included in the global nitrogen/N2O model inter-comparison project phase 2 (NMIP2) (Tian et al., 2024). For each TBM model, anthropogenic fertilizer applications are estimated by the HaNi dataset (Tian et al., 2022), where the fertilizer types (NH<sub>4</sub><sup>+</sup> and NO<sub>3</sub><sup>-</sup>; synthetic fertilizer and manure) are explicitly distinguished in the model. The  $SNO_x$ -Fer can be isolated by summing up the differences between sensitivity experiments SH1 and SH2 (the synthetic fertilizer contribution) and the differences between sensitivity experiments SH1 and SH3 (the manure contribution) (Table S1 in the Supplement). It should be noted that the CLAS-SIC model did not isolate synthetic fertilizer and manure and thus only conducted one sensitivity experiment. The model ensemble mean is utilized to smooth the large discrepancies among different TBMs (Fig. S3) due to the varied terrestrial N-cycle representations, in particular, the varied nitrification and denitrification rates.

# 3 The GEOS-Chem model and sensitivity experiment configuration

The GEOS-Chem model is a frequently used state-of-theart CTM with fully coupled  $NO_x-O_x$ -hydrocarbon-aerosol chemistry mechanism (Bey et al., 2001; Park et al., 2004). Here we applied version 12.0.0 to run the global simulation with a horizontal resolution of 2° latitude ×2.5° longitude. The simulations are driven by the Version two of modern era retrospective-analysis for research and application (MERRA2) reanalyzed meteorological dataset. The photolysis rates were computed by the Fast-JX scheme (Park et al., 2004). The atmospheric gas-phase chemistry is independently developed referring to the kinetics and products based on JPL recommendations (Bates et al., 2024) and solved by the Kinetic Pre-Processor (KPP) (Henze et al., 2007). Aerosol thermodynamic equilibrium is calculated by the ISORROPIA II package (Fountoukis and Nenes, 2007). In particular, the default soil  $NO_x$  emissions are simulated by the BDSNP scheme as introduced above.

In order to examine the uncertainties in  $SNO_x$ -Fer and the associated effects on global surface  $O_3$  concentrations, we first ran a reference simulation in 2019 (named Zero) with zero  $SNO_x$ -Fer to exclude the influence of fertilizer application on soil  $NO_x$ . Then eleven different experiments were performed by representing  $SNO_x$ -Fer with CEDS agricultural  $NO_x$  emissions (named CEDS), the default GEOS-

Chem BDSNP scheme (Eqs. 2–3, named BDSNP\_coarse), the BDSNP scaled by the interannually varied HaNi N fertilizer loadings (Eq. 4, named BDSNP\_coarse\_scaled), the default GEOS-Chem BDSNP but with fine resolution of  $0.5^{\circ} \times$  $0.625^{\circ}$  (named BDSNP\_fine), the TBM-simulated SNO<sub>x</sub>-Fer of each model as well as the ensemble mean (named NMIP2-OCN, NMIP2-CLASSIC, NMIP2-ORCHIDEE and NMIP2, respectively), the linear EF (EF = 1.1%) method (named Linear) and the non-linear EF (Eq. 1) method (named Nonlinear), respectively. In particular, the BDSNP\_fine is simulated offline, i.e., the atmospheric chemical and transport processes are not accounted due to the inconsistency of resolutions with the GEOS-Chem runs. All of the sensitivity experiments are driven by the meteorological field in 2019 with 6-month spin up, where the anthropogenic emissions of all other tracers also keep at the 2019 level following the CEDS inventory. Table 1 summarizes the eleven sensitivity experiments in GEOS-Chem.

In order to further examine the seasonality of  $SNO_x$ -Fer and the associated impacts on ground-level O<sub>3</sub> in agricultural hotspot regions, we investigate how different SNO<sub>x</sub>-Fer approaches distribute the annual fertilizer seasonally (Table 1). The HaNi dataset, as well as the equivalently up-to-date fertilizer dataset (Adalibieke et al., 2023), only provide annual fertilizer application rates given the lack of specific information to distribute N fertilization seasonally. The CEDS, BD-SNP and NMIP2 model approaches have their own specific monthly distribution, while the monthly distribution of fertilizer application in the linear and nonlinear EF is arbitrarily assumed to be even during the growing season. Here, we added two additional GEOS-Chem sensitivity experiments for the linear and non-linear approach, named Linear\_7525 and Nonlinear\_7525, which apply the seasonal pattern of the BDSNP scheme (Hudman et al., 2012), assuming that 75 % of the annual fertilizer is applied in the first month of the growing season and the remaining 25 % evenly applied in the rest of the growing months.

Because the default GEOS-Chem simulations used above do not account for interactive CH<sub>4</sub> chemistry, we further conducted ten more sensitivity experiments with the special "CH<sub>4</sub> run" in GEOS-Chem (East et al., 2024; Fu et al., 2024) to assess variations in the atmospheric CH<sub>4</sub> concentrations induced by the uncertain SNO<sub>x</sub>-Fer. The special CH<sub>4</sub> run takes CH<sub>4</sub> as the sole atmospheric transport tracer with various prescribed CH<sub>4</sub> sources (summarized in Table S2), while the CH<sub>4</sub> sinks include the tropospheric reactions with hydroxyl radical (OH) and chlorine, stratospheric loss and soil uptake. The global monthly mean OH concentrations archived from the ten sensitivity experiments (Table 1, except for the BDSNP\_fine) are applied in the CH<sub>4</sub> simulation to assess the SNO<sub>x</sub>-Fer effect on CH<sub>4</sub> lifetime through perturbing atmospheric oxidation capacity. As a result, there are ten more associated sensitivity experiments with the CH<sub>4</sub> run that correspond to the default GEOS-Chem simulations in Table 1 (except for the BDSNP\_fine experiment). Each CH<sub>4</sub>

**Table 1.** Summary of the sensitivity experiments in GEOS-Chem and the methods used by different  $SNO_x$ -Fer estimating approaches to distribute the annual N fertilizer into monthly.

SNO <sub>x</sub> -Fer estimating approch	Experimental name in this study	Emissions of $SNO_x$ -Fer	Fertilizer monthly distribution	
None	e Zero Zero		None	
Emission Factor (EF)	Linear	Linear EF	Evenly distributed during the growing season	
	Nonlinear	Nonlinear EF		
	Linear_7525	Linear EF	75% of the annual fertilizer is applied in the first month of growing season, while the rest 25% is evenly distributed in the rest growing months	
	Nonlinear_7525	Nonlinear EF		
Emission inventory	CEDS	CEDS agricultural NO <sub>x</sub> sector	Not clear	
BDSNP	BDSNP_coarse	GEOS-Chem default BDSNP with resolution of $2^{\circ} \times 2.5^{\circ}$	75 % of the annual fertilizer is applied in the first month of growing season, while the rest 25 % is evenly distributed in the rest growing months	
	BDSNP_coarse_scaled	BDSNP scaled with the interannual variations of HaNi fertilizer loadings with resolution $2^{\circ} \times 2.5^{\circ}$		
	BDSNP_fine (offline)	GEOS-Chem default BDSNP with resolution of $0.5^{\circ} \times 0.625^{\circ}$	-	
Terrestrial biosphere models (TBMs)	NMIP2-OCN	OCN simulated SNO $_x$ -Fer	Distributed the annual N fertilizer loadings into four equal doses in the first half of the growing season	
	NMIP2-CLASSIC	CLASSIC simulated $SNO_x$ -Fer	Evenly distributed throughout the year in the tropics (between 30° S and 30° N); Evenly distributed from spring equinox to fall equinox between 30° N (30° S) and 90° N (90° S)	
	NMIP2-ORCHIDEE	ORCHIDEE simulated $SNO_X$ -Fer	Half of the annual N fertilizer applied on the first day of the growing season. The remaining half applied on the 30t day since the beginning of the growin season	
	NMIP2	TBMs ensemble mean		

simulation ran for 15 years by repeating the meteorological forcings in 2019 to reach a semi-equilibrium with the prescribed emissions and OH concentrations. The last year of the simulation was utilized to analyze the influences of soil  $NO_x$  on  $CH_4$  induced by N fertilizer application. The simulated global surface  $CH_4$  concentrations driven by varied OH levels from different sensitivity experiments are shown in Fig. S5.

#### 4 Results

## 4.1 Varied SNO<sub>x</sub>-Fer among different approaches

Figure 1 shows the historical time series of global SNO<sub>x</sub>-Fer over 1950–2019 estimated by different approaches, mainly driven by the substantial increases in global N fertilizer application. Almost all approaches except BDSNP showed enhancements in soil NO<sub>x</sub> emissions but with largely varied magnitudes from 0.6 to 2.1 Tg yr<sup>-1</sup> over 1950–2019. The default BDSNP scheme in GEOS-Chem, which scales soil NO<sub>x</sub>

#### Fertilizer-induced soil NO<sub>x</sub> emissions

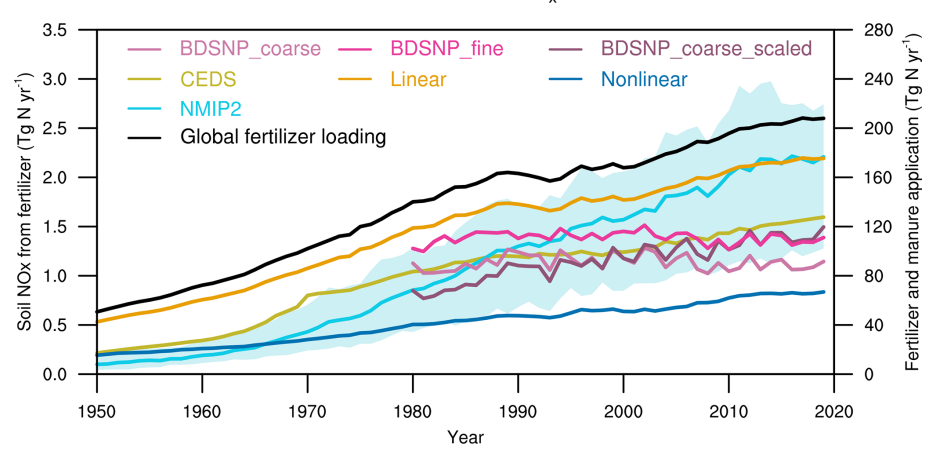


Figure 1. Global estimates of N fertilizer-induced soil NO<sub>x</sub> emissions by different approaches. The black line (right Y axis) indicates global annual-mean N synthetic fertilizer and manure inputs over 1950–2019 assessed from the HaNi dataset. The remaining lines (left Y axis) indicate the N fertilizer-induced soil NO<sub>x</sub> emissions over 1950–2019 estimated by different approaches, including the emission inventory (CEDS), linear and non-linear EF, the widely-used CTM parameterization with coarse resolution ( $2^{\circ} \times 2.5^{\circ}$ , BDSNP\_coarse), fine resolution ( $0.5^{\circ} \times 0.625^{\circ}$ , BDSNP\_fine) and interannually varied N availability (BNDSP\_coarse\_scaled), and the TBM ensembles (NMIP2). The light cyan shadows indicate the spread across three different TBMs in NMIP2.

emissions with time-variant temperature and soil moisture, but assumes constant N availability (see Methods), estimates relatively stable soil  $NO_x$  emissions over 1980–2019. The annually-varied BDSNP scheme scaled by the HaNi N input dataset shows an increase in  $SNO_x$ -Fer from 0.8 Tg N yr<sup>-1</sup> in 1980 to 1.5 Tg N yr<sup>-1</sup> in 2019, while the sharpest increase in the soil  $NO_x$  emission is simulated by the TBM ensemble, mainly induced by the high estimates of the CLASSIC and ORCHIDEE models (Fig. S3). Soil  $NO_x$  estimated by the non-linear EF approach shows a substantially weaker response to fertilizer inputs relative to other estimating approaches.

Figure 3 shows the global spatial patterns of SNO<sub>x</sub>-Fer among different approaches. Each approach shows consistent spatial patterns aligned with the distribution of N synthetic fertilizer and manure inputs (Fig. 2), where eastern U.S., western Europe, eastern and southern Asia are the hotspots with high soil  $NO_x$  emissions. Notably, even though the TBM ensemble (NMIP2) and the Linear EF approach estimate similar global total SNO<sub>x</sub>-Fer, the spatial distributions of both estimates vary strongly. The SNO<sub>x</sub>-Fer estimates from the NMIP2 ensemble are higher in agricultural hotspots (Table 2), but lower in regions with less synthetic fertilizer application, e.g. in parts of the Africa and South America (Fig. 3d and e), relative to the Linear EF approach. It is because plants and microbes have high priority to assess additional N in N-limited regions, which leads less N loss as the gas forms. However, in N-saturated regions, the applied N fertilizer is excessive for the living biomes, yielding a higher sensitivity of soil  $NO_x$  emissions to N fertilizer application (Du and de Vries, 2025). Such N dynamics have been included in the C-N fully-coupled TBMs, but are not represented by the linear EF approach.

# 4.2 The seasonal cycle of $SNO_X$ -Fer and the associated impact on $O_3$ concentrations

Figure 4 shows the seasonality of  $SNO_x$ -Fer in four agricultural hotspot regions among different SNO<sub>x</sub>-Fer estimating methods. In the temperate regions like Eastern U.S., Western Europe and Eastern Asia, the TBM ensemble NMIP2 shows very strong seasonal variations, which peaks during May to July in Eastern U.S., April to June in Western Europe and May to August in Eastern Asia, respectively. The seasonality of the linear and nonlinear EF methods is strongly dependent on the assumption of fertilizer application time (Table 1), where the monthly  $SNO_x$ -Fer emissions are at similar levels during the growing season for the Linear and Nonlinear experiments, but peak in a pronounced manner in the northern-hemispheric springtime (around February to April) in the Linear\_7525 and Nonlinear\_7525 cases. Although the BDSNP applies the same assumption of fertilizer application time as Linear\_7525 and Nonlinear\_7525, the SNO<sub>x</sub>-Fer in BDSNP peaks much later (September to October in Eastern U.S., June to August in Western Europe and May to June in Eastern Asia). This arises because the EF methods estimate SNO<sub>x</sub>-Fer instantaneously in response to the fertilizer application, but the BDSNP scheme cumulates N fertilizer with a 4-month time window (Eq. 3). It is also very important the BDSNP includes the regulation of soil temperature and moisture on SNO<sub>x</sub>-Fer, both of which also have strong seasonality, but the EF methods do not. Furthermore, in the tropical regions of southern Asia, the NMIP2, Linear\_7525 and

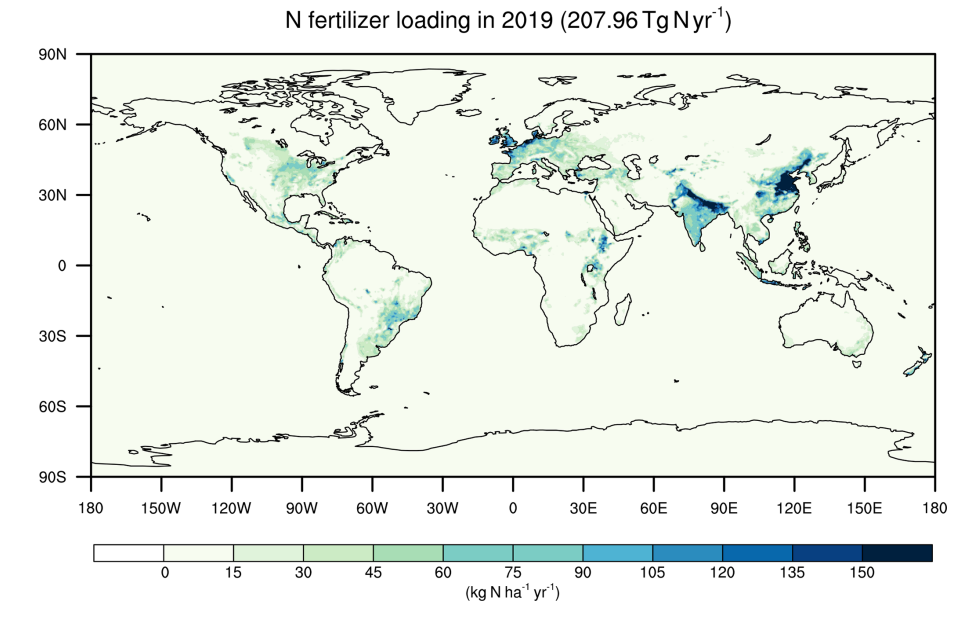


#### Figure 2. The global spatial patterns of N synthetic fertilizer and manure application in 2019 from the HaNi dataset.

**Table 2.** The annual soil  $NO_x$  emissions  $(Gg \, N \, yr^{-1})$  induced by N fertilizer in 2019 in the eastern U.S., western Europe, eastern Asia, southern Asia and the global estimates by different approaches. The ranges in NMIP2 indicate the highest and lowest values among three TBMs (CLASSIC, ORCHIDEE and OCN).

	Eastern U.S. (35–45° N, 75–90° W)	Western Europe (35–60° N, 10° W–20° E)	Eastern Asia (20–50° N, 100–125° E)	Southern Asia (10–30° N, 70–85° E)	Globe
CEDS	20.9	99.1	190.0	104.8	1600
BDSNP_corase	15.8	76.3	157.0	134.2	1150
BDSNP_corase_scaled	17.6	69.8	174.8	201.7	1500
NMIP2	57.0 [15.1,	206.3 [67.4,	417.5 [261.0,	382.4 [78.4,	2210 [1280,
	100.9]	267.3]	598.1]	776.3]	2740]
Linear EF	54.3	181.0	376.4	214.7	2190
Non-Linear EF	15.6	60.8	136.5	141.8	840

Nonlinear\_7525 experiments estimate the peak  $SNO_x$ -Fer in the beginning of the year, while the  $SNO_x$ -Fer of BDSNP reaches its highest in May due to the N cumulation assumption (Fig. 4d). The remaining methods, including the emissions inventory CEDS, the Linear and Nonlinear EF method, show very weak seasonality of  $SNO_x$ -Fer in Southern Asia.

The seasonality of ground-level monthly MDA8  $O_3$  changes in response to the SNO<sub>x</sub>-Fer in general aligns with the monthly variations of SNO<sub>x</sub>-Fer among different estimating approaches (Fig. 5). The strongest enhancement of regional MDA8  $O_3$  occurs during the northern-hemispheric summertime (June–August) for most of the estimating approaches in three temperate regions, when the absolute  $O_3$  concentrations also reaches their highest. However, it should be noted that spring-peak SNO<sub>x</sub>-Fer in the Linear\_7525 and the Nonlinear\_7525 cases does not lead to high  $O_3$  enhancement in both western Europe and eastern Asia (Fig. 5b and c).

The weak sensitivity of  $O_3$  to  $NO_x$  during springtime is likely the result of the seasonal variations in other emissions (e.g. biogenic volatile organic compounds (BVOCs)), which alter the chemical sensitivity regime. The responses of  $O_3$  to  $SNO_x$ -Fer could also depend on the region (e.g.  $O_3$  enhancement also peaks during spring in Linear\_7525 in Eastern U.S., Fig. 5a), spatial simulation resolution or different modelling chemical mechanisms. The  $O_3$  enhancement in southern Asia is generally similar during northern-hemispheric spring and summer time for all of the  $SNO_x$ -Fer estimating approaches (Fig. 5d), except for the BDSNP scheme, which simulates significantly higher  $O_3$  enhancement during May to July relative to February to April.

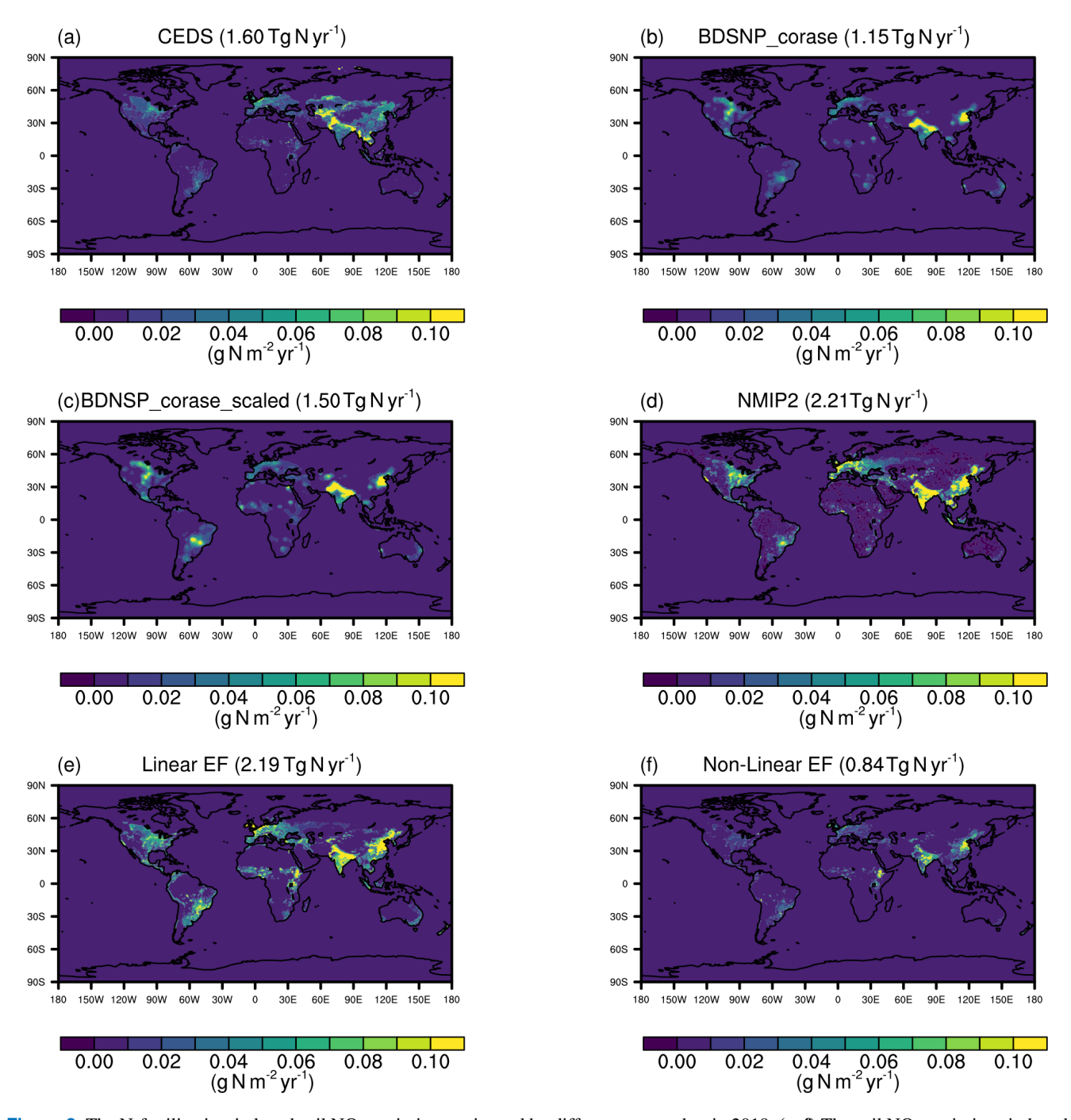


**Figure 3.** The N-fertilization-induced soil  $NO_x$  emissions estimated by different approaches in 2019. (a–f) The soil  $NO_x$  emissions induced by N fertilizer estimated by the CEDS agricultural sector, the default BDSNP scheme in GEOS-Chem with coarse resolution ( $2^{\circ} \times 2.5^{\circ}$ ), the coarse-resolution BDSNP scheme in GEOS-Chem by interannually scaling the N availability using the HaNi dataset, the NMIP2 ensemble, the linear EF and non-linear EF, respectively. The global total budget of each estimate is given in the subtitles.

## 4.3 Impacts of $SNO_X$ -Fer on surface $O_3$ concentrations

We next examine how the different  $SNO_x$ -Fer estimates influence the surface  $O_3$  concentrations globally. Since soil  $NO_x$  emissions typically peak during the summer period (Fig. 4), when  $O_3$  pollution tends to be most severe, we fo-

cus our analysis on the surface maximum daily 8 h averaged (MDA8) O<sub>3</sub> concentrations averaged over the northern hemisphere summer (June, July and August) based on the sensitivity experiments in Table 1. Figure 6 shows that the N fertilizer application enhanced the globally-averaged surface summertime O<sub>3</sub> MDA8 concentrations by 0.04–0.30 ppbv in

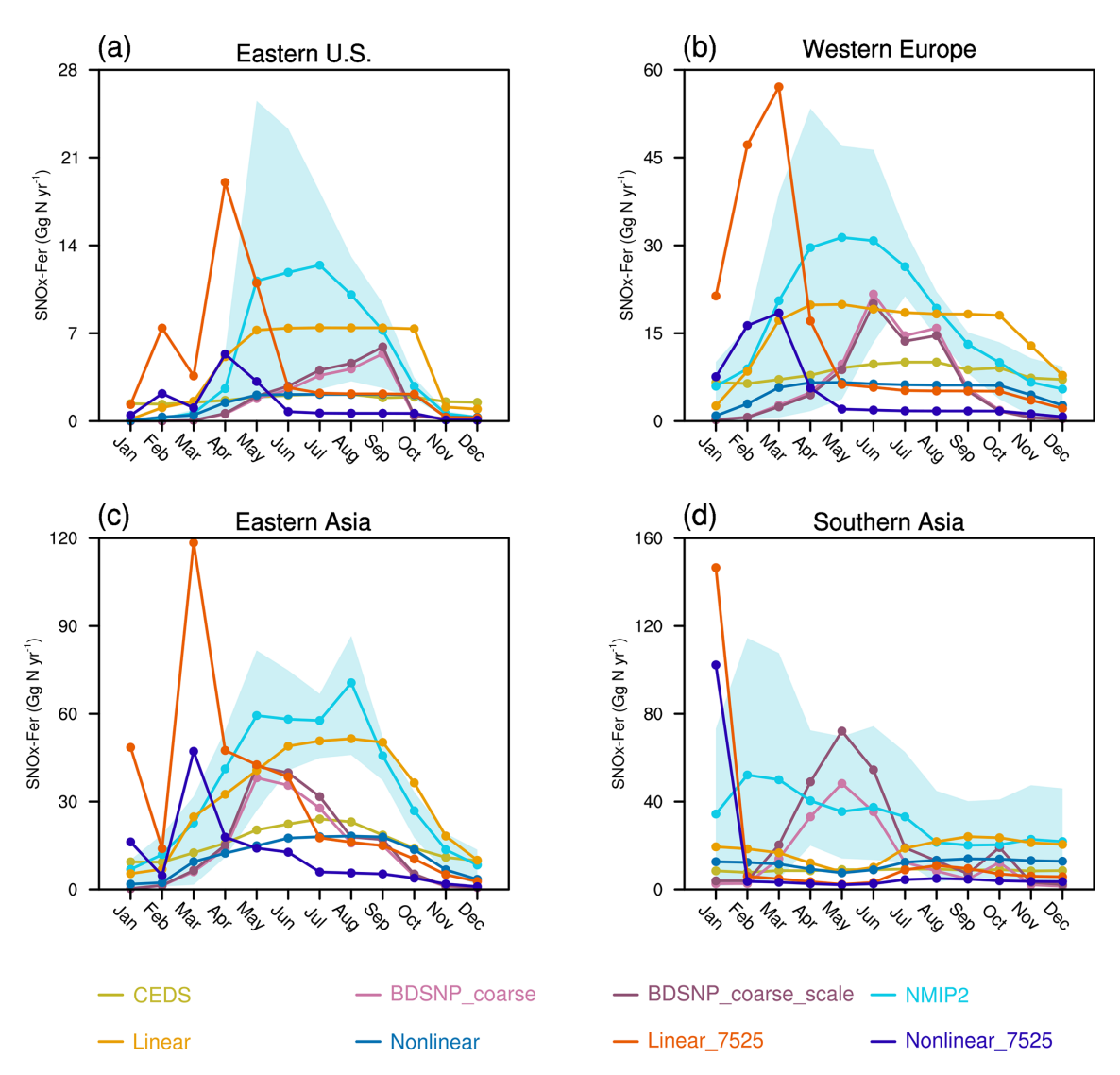


Figure 4. The monthly regional SNO<sub>x</sub>-Fer (Gg N yr<sup>-1</sup>) in (a) eastern U.S., (b) western Europe, (c) eastern Asia and (d) southern Asia with different SNO<sub>x</sub>-Fer estimating approaches. The cyan-blue shades indicate the spread among three different TBM models (CLASSIC, OCN and ORCHIDEE) in the NMIP2 ensemble.

2019. In agricultural regions, the enhancement of  $O_3$  concentrations due to  $SNO_x$ -Fer reaches 0.1–3.3 ppbv (0.2%–7.0%). Figure 6 also highlights important differences in the spatial effect of  $NO_x$  on  $O_3$ , consistent with the regional effects on  $SNO_x$ -Fer (Table 2), that the NMIP2 estimate of  $SNO_x$ -Fer shows stronger contributions to the  $O_3$  concentrations than the linear EF approach in agricultural regions. The non-linear EF method leads to the lowest  $O_3$  enhancement, although both non-linear EF and TBMs estimate increasing soil  $NO_x$  emissions with soil N availability.

# 4.4 The impacts of $SNO_X$ -Fer uncertainties on global $CH_4$ estimates

Figure 7 shows that N fertilizer-induced soil  $NO_x$  led to the reduction of globally averaged  $CH_4$  concentrations ranging from 6.7 ppbv (0.4%) to 16.6 ppbv (0.9%) in 2019 by increasing atmospheric OH concentrations (Fig. S5), spatially aligned with the distributions of  $SNO_x$ -Fer among different estimating approaches (Fig. 3). Because  $CH_4$  has a significantly longer atmospheric lifetime than either OH or  $NO_x$ , the spatial differences in the impacts of  $SNO_x$ -Fer on  $CH_4$  concentrations are insignificant (Fig. S4). As a result, we only focus on the globally averaged changes in  $CH_4$  concentrations. The magnitude of this estimate is consistent with the recent estimate of around 17.4 ppbv by Gong et al. (2024), which relies on the same NMIP2 dataset and a simpler  $CH_4$ 

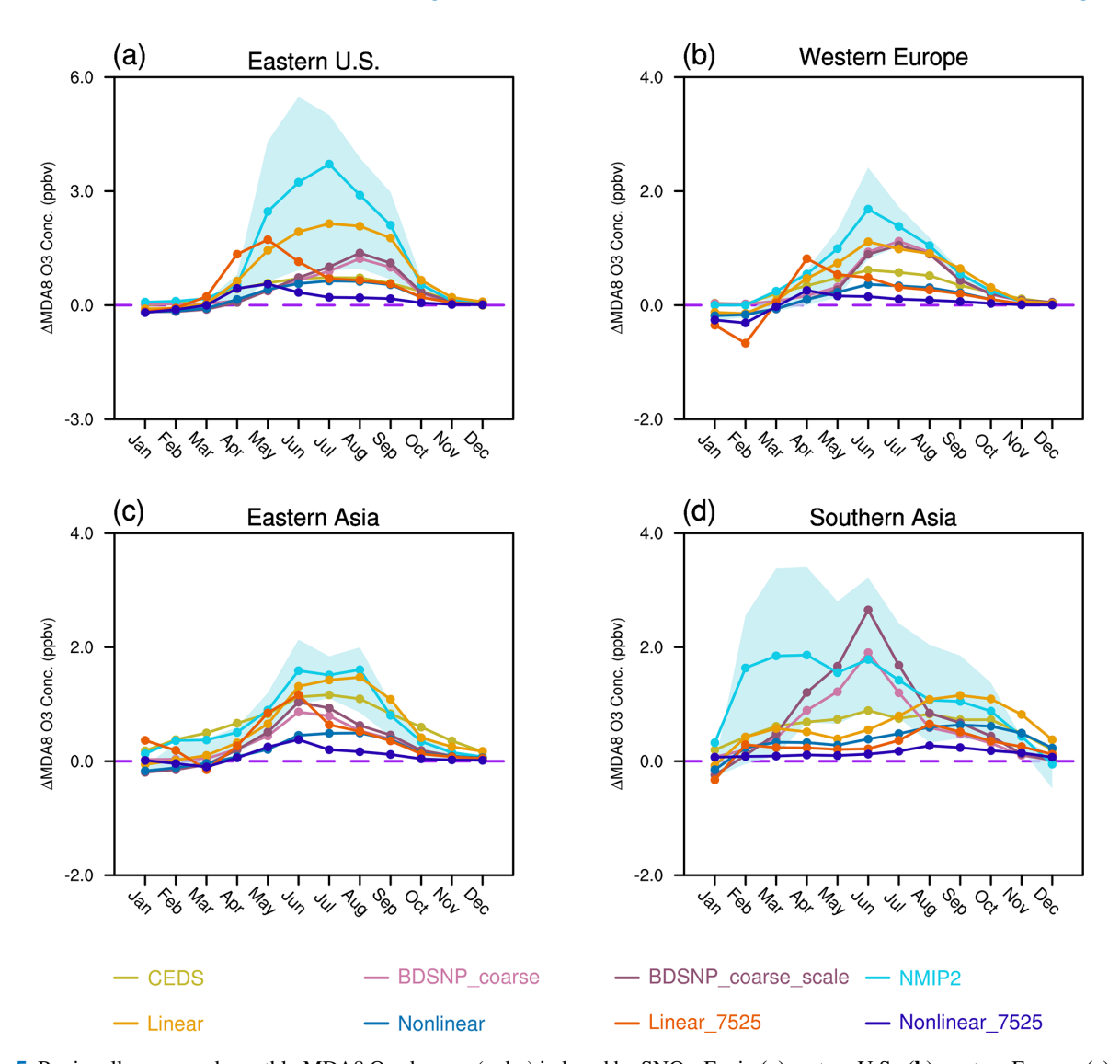


Figure 5. Regionally-averaged monthly MDA8  $O_3$  changes (ppbv) induced by SNO<sub>x</sub>-Fer in (a) eastern U.S., (b) western Europe, (c) eastern Asia and (d) southern Asia with different SNO<sub>x</sub>-Fer estimating approaches. The cyan-blue shades indicate the spread among three different TBM models (CLASSIC, OCN and ORCHIDEE) in the NMIP2 ensemble.

box model to calculate the impacts of  $NO_x$  emissions on the atmospheric lifetime of  $CH_4$ . This result highlights an important but indirect role of  $SNO_x$ -Fer on atmospheric  $CH_4$  concentrations, which is an often-overlooked aspect for the global  $CH_4$  budget. However, the uncertainty range in our estimates clearly suggests the need to further improve our understanding of soil N biogeochemical processes to better predict global OH reactivity and to better constrain global  $CH_4$  budget.

#### 5 Discussions

In this study, we integrated knowledge from meta-analyses (Buendia et al., 2019; Wang et al., 2024), the emission inventory, parameterizations in CTMs and the TBM ensembles

to better quantify the uncertainties in N fertilizer-induced soil  $NO_x$  emissions and the associated impacts on global  $O_3$  and  $CH_4$  concentrations. Our results showed a large variation in the global soil  $NO_x$  emissions associated with N fertilizer, ranging from 0.84 to  $2.2\,\mathrm{Tg}\,\mathrm{N}\,\mathrm{yr}^{-1}$  in 2019. This range of responses leads to an enhancement in summertime surface MDA8  $O_3$  concentrations of 0.1 to  $3.3\,\mathrm{ppbv}$  ( $0.2\,\%$ – $7.0\,\%$ ) in agricultural hotspot regions. The  $O_3$  enhancement is highest in eastern U.S., while it is not only determined by the  $SNO_x$ -Fer emissions, but also the diverging sensitivities of  $O_3$  to  $NO_x$  depending on different chemical regimes in GEOS-Chem (Fig. S6). The varied  $SNO_x$ -Fer estimates also lead to a reduction in global  $CH_4$  concentrations of  $6.7\,\mathrm{ppbv}$  ( $0.4\,\%$ ) to  $16.6\,\mathrm{ppbv}$  ( $0.9\,\%$ ). These changes highlight a significant role of agricultural N use and soil N biogeochemical

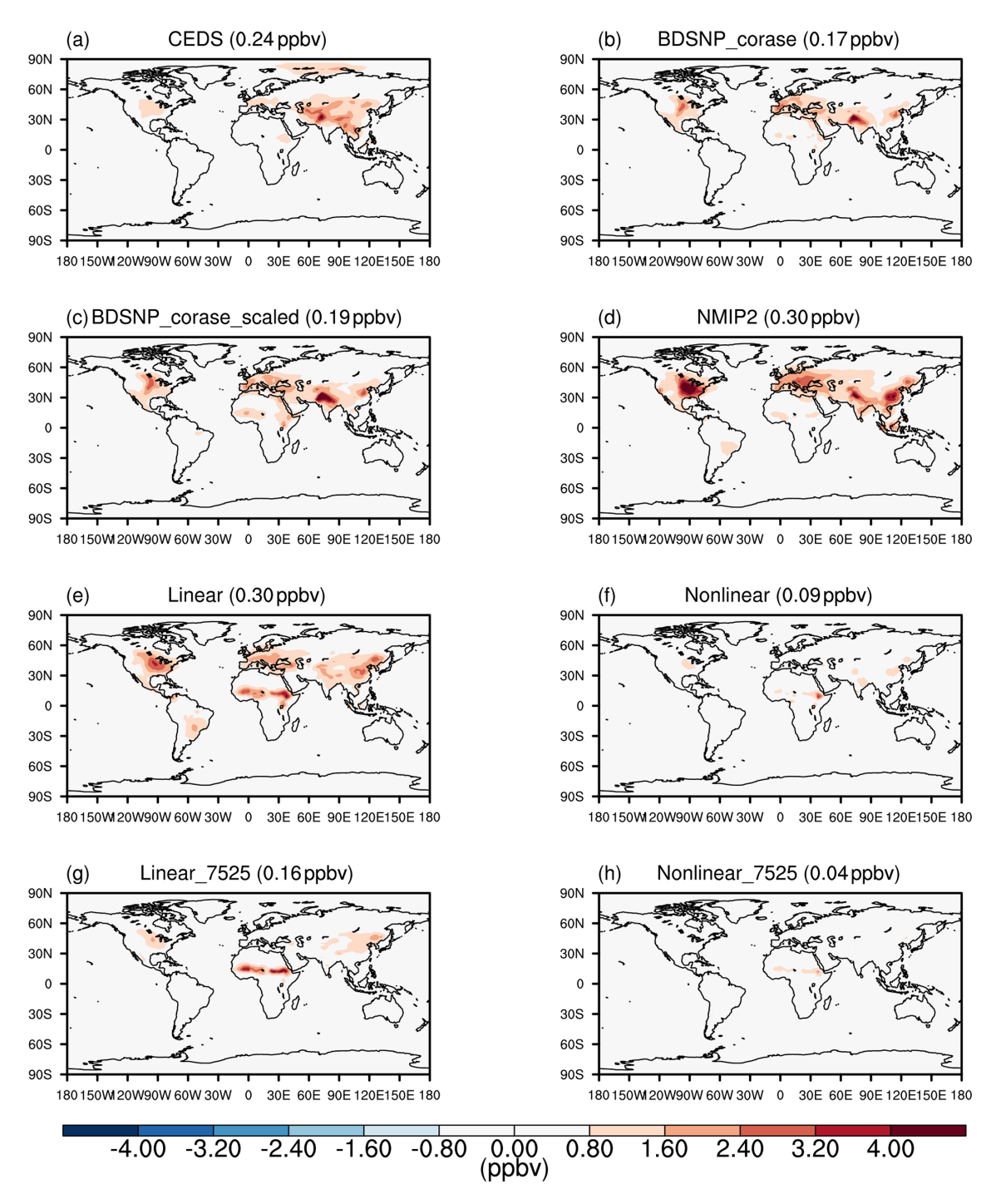


Figure 6. Global simulated changes in surface MDA8  $O_3$  concentrations induced by different estimating approaches of SNO<sub>x</sub>-Fer averaged over June, July and August in 2019. The differences are calculated between corresponding sensitivity experiments in Table 1 and the Zero experiment. The numbers in each subtitle are changes in the globally averaged summertime MDA8  $O_3$  concentrations induced by SNO<sub>x</sub>-Fer.

processes in affecting regional  $O_3$  concentrations as well as controlling global greenhouse gases. In particular, with the worldwide reduction in fossil-fuel  $NO_x$  emissions associated with clean-air actions (Jiang et al., 2022), control of agricultural soil  $NO_x$  emissions becomes increasingly important to

improve air quality and alleviate the associated public health risks.

However, challenges remain in the accurate assessment of N fertilizer-induced soil  $NO_x$  emissions. On the one hand, the overall uncertainties of  $SNO_x$ -Fer may still be underesti-

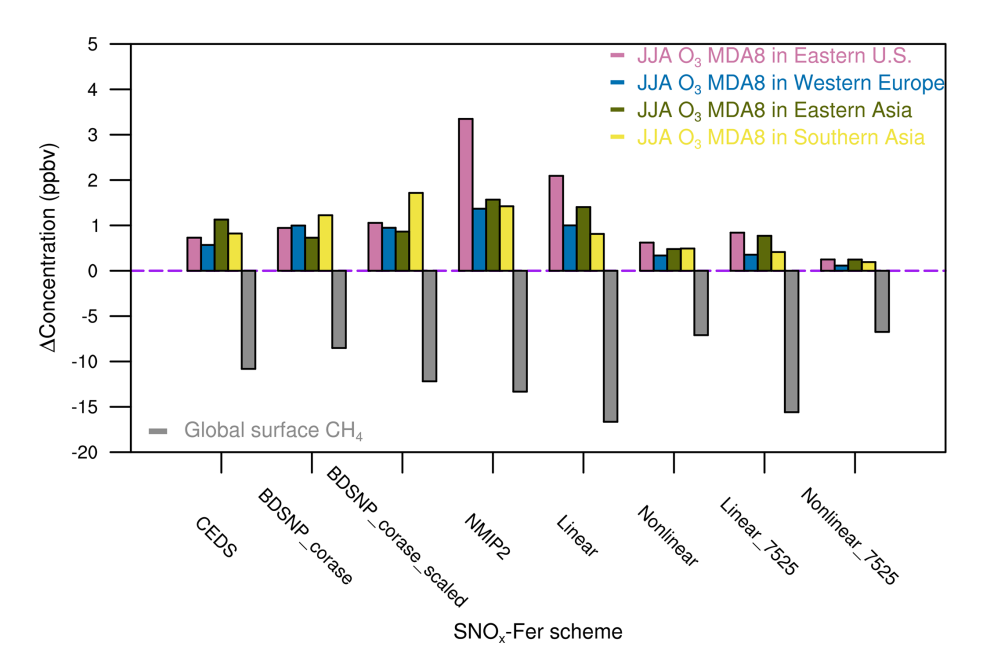


Figure 7. Changes in summertime averaged surface MDA8  $O_3$  concentrations (positive Y axis) and global surface CH<sub>4</sub> concentrations (negative Y axis) induced by SNO<sub>x</sub>-Fer uncertainties. The regional MDA8  $O_3$  concentrations are averaged over eastern U.S. (35–45° N, 75–90° W), western Europe (35–60° N, 10° W–20° E), eastern Asia (20–50° N, 100–125° E) and southern Asia (10–30° N, 70–85° E).

mated. The EF-approach with fixed EF fails to adequately reflect the complexity in soil biogeochemical processes, which is reflected by the large ranges of EFs from 0.06 % to 2.18 % in a recent meta-analysis (Buendia et al., 2019). While the non-linear EF method represents an advance over the linear EF approach, as the effects of soil N saturation levels on soil N gas emissions are considered and therefore the approach yields relatively good performance in predicting soil N<sub>2</sub>O or NH<sub>3</sub> emissions compared to observations (Shcherbak et al., 2014; Jiang et al., 2017), the limited availability of observations to constrain these responses and their limited spatiotemporal representativeness reduce the reliability of this approach. Most of the experimental data in Wang et al. (2024) are collected over China in the past ten years and thus may not be representative of other agricultural regions. Furthermore, 22 out of 55 data points are from vegetable cropping systems and orchard fields, where frequent irrigation may enhance soil moisture and thus inhibit the production of  $NO_x$  via nitrification. Last but not least, other factors, such as soil texture, pH, soil organic carbon and fertilizer types, may also affect the response of soil  $NO_x$  emissions to the loading of N fertilizer application, which are omitted by either the linear EF or non-linear EF approach. As a result, more representative crop experiments with a gradient series of N addition are necessary to better constrain the soil  $NO_x$ response to N fertilizer application.

For the modelling of  $SNO_x$ -Fer, on the one hand, recent developments of the parameterization of BDSNP in CTMs focused more on the soil  $NO_x$  responses to changing temperature or soil moisture (e.g. Wang et al., 2021; Huber et al.,

2023), while the accuracy of the soil N availability has been less investigated. Even with the scaled N fertilizer loadings to interannually vary the N availability, BDSNP still showed a weaker increasing trend of  $SNO_x$ -Fer in response to the N fertilizer enhancement relative to the empirical EF methods and the TBM simulations of NMIP2 in the past decades (Fig. 1). Nevertheless, it should be noted that the BDSNP scheme is also sensitive to the spatial resolution, where the coarse resolution may miss small-scale hotspots and thus underestimate the global SNO $_x$ -Fer, as the BDSNP\_fine experiment shows in Fig. 1. On the other hand, terrestrial N availability is a key concept in the development of TBMs, as the process-based TBMs need a detailed description of the N cycle to understand nutrient limitation levels and associated C-N coupling. Nevertheless, the soil  $NO_x$  emissions have been overlooked by the ecological modelling community because the low emissions may not be important for the terrestrial N cycle, resulting in a limited number of TBMs that include soil NO<sub>x</sub> emissions as well as large inter-model variations (Fig. S3). To further reduce the uncertainties in soil  $NO_x$ emission estimates, the advantages of TBMs on representing soil N availability can be introduced into CTMs to better examine the effects of agricultural activities on atmospheric chemistry, but at the same time, the terrestrial N cycle needs to be further developed in TBMs to reduce inter-model variations and to better predict soil emissions of reactive N gases (not only  $NO_x$  but also  $N_2O$  and  $NH_3$ ).

The seasonality of  $SNO_x$ -Fer and the associated impacts on surface  $O_3$  concentrations are also important but poorly constrained. The most difficult challenge is to precisely es-

timate the monthly (or even daily) N fertilizer loadings on the global scale. Because the N fertilizer data underlying the gridded products is derived from the annual statistics by the Food and Agricultural Organization (FAO) (https://www. fao.org/faostat/en/#data, last access: 24 November 2025), the HaNi dataset applied in this study, as well as the equivalently up-to-date fertilizer dataset (Adalibieke et al., 2023), only provides gridded, annual fertilizer application rates. In the EF approaches, the growing season is determined only by temperature and greenness in this study, which could result in a mismatch with the real crop or pasture calendar, especially ignoring the multiple-harvest crops per year. A refined calendar could further improve the prediction of SNO<sub>x</sub>-Fer seasonality. Furthermore, the NO<sub>x</sub>-VOCs-O<sub>3</sub> chemical sensitivity regimes could be determined not only by soil  $NO_x$  emissions, but also by other anthropogenic and biogenic emissions of  $NO_x$  and VOCs, as well as the climate seasonal variations. Therefore, the seasonal cycles of the enhancement of O<sub>3</sub> concentrations may not strictly follow the variations in  $SNO_x$ -Fer, as our Linear\_75 sensitivity experiment implies in Western Europe and Eastern Asia (Fig. 5b and c).

The impacts of the changes in short-lived air pollutants on the global CH<sub>4</sub> budget have attracted increasing attention in recent years (Peng et al., 2022; Zhao et al., 2025), where  $NO_x$ is one of the most important drivers. However, it should be noted that the sensitivity of  $CH_4$  lifetime to  $NO_x$  emissions varies substantially among atmospheric chemistry models from -25% to -46% in response to the total NO<sub>x</sub> changes from the pre-industrial to present-day period (Thornhill et al., 2021). Because few studies investigated how  $NO_x$  from agricultural sources affects CH<sub>4</sub>, it is difficult to assess if the overall impacts of SNO<sub>x</sub>-Fer on CH<sub>4</sub> presented in this study based on the GEOS-Chem model are underestimated or overestimated, even though certain uncertainties are expected. Nevertheless, our results indicate that SNO<sub>x</sub>-Fer could be an uncertain but important source in calculating future changes of the global CH<sub>4</sub> budget, the importance of which could increase with future continuing reduction in fossil-fuel NO<sub>x</sub> emissions (Rao et al., 2017)

Beyond the uncertainties remaining in different SNO<sub>x</sub>-Fer estimating approaches, an important but also difficult question is how to better evaluate the performances of each method, especially at the regional and global scales. The first-hand meta-data collected from the field experiments is actually not an independent source, as it has been used to establish both of the linear and nonlinear EF methods. More importantly, most of the field experiments are manipulation experiments with artificial fertilizer gradients, which may not fully represent the real-world spatiotemporally varied SNO<sub>x</sub>-Fer. Furthermore, we use O<sub>3</sub> data from the national or continental air quality observational networks to evaluate simulated O<sub>3</sub> concentrations as a potential consistency check of the SNO<sub>x</sub>-Fer (Fig. S7). However, the uncertainties in SNO<sub>x</sub>-Fer are expected to be far less important relative to the uncertainties in the nonlinearity of atmospheric chemistry, emissions of BVOCs or the deposition processes, which together determine the biases between observational and simulated O<sub>3</sub> concentrations. As a result, it is inappropriate to determine the best  $SNO_x$ -Fer estimate as the one with the best statistical metrics in O<sub>3</sub> simulation. Moreover, most of the sites that monitor air pollutants are located in the urban regions, where the industrial impacts are far more important than the agricultural sources. A real-time O<sub>3</sub> observational network in the cropland or pasture would be crucial to advance the understandings in  $SNO_x$ -Fer and the associated impacts on air quality. Last but not least, the top-down retrievals of  $NO_x$ emissions based on satellite NO<sub>2</sub> products could also have the potential to better constrain  $SNO_x$ -Fer, while gaps remain in how to precisely isolate the soil  $NO_x$  emissions (Bertram et al., 2005; Lin et al., 2024) and even the fertilizer contributions from the total  $NO_x$  sources. Synergizing spatiotemporally detailed fertilizer management datasets with the topdown NO<sub>x</sub> retrievals with ultra-high resolutions, where the atmospheric  $NO_x$  can be assumed to be dominantly affected by the soil sources in agricultural regions, could be one possible solution. However, more work is needed to integrate such big data in the future.

To summarize, with a comprehensive investigation of different approaches to describe  $SNO_x$ -Fer, our results reveal the uncertainties in quantifying  $SNO_x$ -Fer and the associated important implications in simulating regional air quality and the global greenhouse gas  $CH_4$ . However, the limited number of field experiments impedes accurate assessments of the soil  $NO_x$  responses to N fertilizer application as well as improving its representation in both CTMs and TBMs, resulting in large uncertainties in estimates of N fertilizer-induced soil  $NO_x$  emissions. We thus highlight the essential necessity to integrate knowledge between agricultural data, atmospheric chemistry modelling and soil biogeochemistry to better represent soil  $NO_x$  emissions in models and improve our understanding of the associated effects on air quality and the global  $CH_4$  budget.

Code and data availability. The GEOS-Chem source code can be assessed at https://github.com/geoschem/geos-chem (last access: 24 November 2025). The CEDS inventory used in GEOS-Chem can be downloaded from http://geoschemdata.wustl.edu/ExtData/HEMCO/CEDS/ (last access: 24 November 2025). The NMIP2 model outputs can be downloaded through the open-accessed data in Gong et al. (2024).

**Supplement.** The supplement related to this article is available online at https://doi.org/10.5194/acp-25-17009-2025-supplement.

**Author contributions.** C.G. designed the study. C.G. performed the GEOS-Chem simulations and data analysis. Y.W. helps the nonlinear EF analysis. H.T. led the NMIP2 projects. S.K, N.V., and S.Z. together contributed to the simulation of terrestrial biosphere mod-

els in NMIP2. C.G. wrote the manuscript. All of the authors contributed to reviewing or editing the manuscript.

**Competing interests.** The contact author has declared that none of the authors has any competing interests.

**Disclaimer.** Publisher's note: Copernicus Publications remains neutral with regard to jurisdictional claims made in the text, published maps, institutional affiliations, or any other geographical representation in this paper. While Copernicus Publications makes every effort to include appropriate place names, the final responsibility lies with the authors. Views expressed in the text are those of the authors and do not necessarily reflect the views of the publisher.

**Financial support.** This research has been supported by the H2020 European Research Council (grant no. 101003536).

The article processing charges for this open-access publication were covered by the Max Planck Society.

**Review statement.** This paper was edited by Rebecca Garland and reviewed by three anonymous referees.

#### References

- Adalibieke, W., Cui, X. Q., Cai, H. W., You, L. Z., and Zhou, F.: Global crop-specific nitrogen fertilization dataset in 1961–2020, Scientific Data, 10, https://doi.org/10.1038/s41597-023-02526-z, 2023.
- Bates, K. H., Evans, M. J., Henderson, B. H., and Jacob, D. J.: Impacts of updated reaction kinetics on the global GEOS-Chem simulation of atmospheric chemistry, Geosci. Model Dev., 17, 1511–1524, https://doi.org/10.5194/gmd-17-1511-2024, 2024.
- Bertram, T. H., Heckel, A., Richter, A., Burrows, J. P., and Cohen, R. C.: Satellite measurements of daily variations in soil NOx emissions, Geophysical Research Letters, 32, L24812, https://doi.org/10.1029/2005gl024640, 2005.
- Bey, I., Jacob, D. J., Yantosca, R. M., Logan, J. A., Field, B. D., Fiore, A. M., Li, Q. B., Liu, H. G. Y., Mickley, L. J., and Schultz, M. G.: Global modeling of tropospheric chemistry with assimilated meteorology: Model description and evaluation, Journal of Geophysical Research-Atmospheres, 106, 23073–23095, https://doi.org/10.1029/2001jd000807, 2001.
- Buendia, E. C., Tanabe, K., Kranjc, A., Baasansuren, J., Fukuda, M., Ngarize, S., Osako, A., Pyrozhenko, Y., Shermanau, P., and Federici, S.: Refinement To the 2006 Ipcc Guidelines for National Greenhouse Gas Inventories, IPCC, Geneva, Switzerland, https://www.ipcc-nggip.iges.or.jp/public/2019rf/pdf/0\_Overview/19R\_V0\_00\_Cover\_Foreword\_Preface\_Dedication.pdf (last access: 26 November 2025), 2019.
- Cheng, W. G., Tsuruta, H., Chen, G. X., and Yagi, K.: N2O and NO production in various Chinese agricultural soils by nitrification, Soil Biology & Biochemistry, 36, 953–963, https://doi.org/10.1016/j.soilbio.2004.02.012, 2004.

- Delmas, R., Serca, D., and Jambert, C.: Global inventory of NOx sources, Nutrient Cycling in Agroecosystems, 48, 51–60, https://doi.org/10.1023/a:1009793806086, 1997.
- Du, E. Z. and de Vries, W.: Links Between Nitrogen Limitation and Saturation in Terrestrial Ecosystems, Global Change Biology, 31, https://doi.org/10.1111/gcb.70271, 2025.
- East, J. D., Jacob, D. J., Balasus, N., Bloom, A. A., Bruhwiler, L., Chen, Z. C., Kaplan, J. O., Mickley, L. J., Mooring, T. A., Penn, E., Poulter, B., Sulprizio, M. P., Worden, J. R., Yantosca, R. M., and Zhang, Z.: Interpreting the Seasonality of Atmospheric Methane, Geophysical Research Letters, 51, https://doi.org/10.1029/2024g1108494, 2024.
- Eggleston, H., Buendia, L., Miwa, K., Ngara, T., and Tanabe, K.: 2006 IPCC guidelines for national greenhouse gas inventories, Institute for Global Environmental Strategies (IGES), https://www.ipcc.ch/report/2006-ipcc-guidelines-for-national-greenhouse-gas-inventories/(last access: 26 November 2025), 2006.
- Erisman, J. W., Galloway, J., Seitzinger, S., Bleeker, A., and Butterbach-Bahl, K.: Reactive nitrogen in the environment and its effect on climate change, Current Opinion in Environmental Sustainability, 3, 281–290, https://doi.org/10.1016/j.cosust.2011.08.012, 2011.
- Fleischer, K., Dolman, A. J., van der Molen, M. K., Rebel, K. T., Erisman, J. W., Wassen, M. J., Pak, B., Lu, X. J., Rammig, A., and Wang, Y. P.: Nitrogen Deposition Maintains a Positive Effect on Terrestrial Carbon Sequestration in the 21st Century Despite Growing Phosphorus Limitation at Regional Scales, Global Biogeochemical Cycles, 33, 810–824, https://doi.org/10.1029/2018gb005952, 2019.
- Fountoukis, C. and Nenes, A.: ISORROPIA II: a computationally efficient thermodynamic equilibrium model for K<sup>+</sup>–  $Ca^{2+}$ – $Mg^{2+}$ – $NH_4^+$ – $Na^+$ – $SO_4^2$ – $NO_3^-$ – $Cl^-$ – $H_2O$  aerosols, Atmos. Chem. Phys., 7, 4639–4659, https://doi.org/10.5194/acp-7-4639-2007, 2007.
- Fowler, D., Coyle, M., Skiba, U., Sutton, M. A., Cape, J. N., Reis, S., Sheppard, L. J., Jenkins, A., Grizzetti, B., Galloway, J. N., Vitousek, P., Leach, A., Bouwman, A. F., Butterbach-Bahl, K., Dentener, F., Stevenson, D., Amann, M., and Voss, M.: The global nitrogen cycle in the twenty-first century, Philosophical Transactions of the Royal Society B-Biological Sciences, 368, https://doi.org/10.1098/rstb.2013.0164, 2013.
- Fu, B., Li, J. Y., Jiang, Y. Y., Chen, Z. W., and Li, B. A.: Clean air policy makes methane harder to control due to longer lifetime, One Earth, 7, https://doi.org/10.1016/j.oneear.2024.06.010, 2024.
- Goldberg, D. L., Harkey, M., de Foy, B., Judd, L., Johnson, J., Yarwood, G., and Holloway, T.: Evaluating NOx emissions and their effect on O3 production in Texas using TROPOMI NO2 and HCHO, Atmos. Chem. Phys., 22, 10875–10900, https://doi.org/10.5194/acp-22-10875-2022, 2022.
- Gong, C., Liao, H., Zhang, L., Yue, X., Dang, R. J., and Yang, Y.: Persistent ozone pollution episodes in North China exacerbated by regional transport, Environmental Pollution, 265, https://doi.org/10.1016/j.envpol.2020.115056, 2020.
- Gong, C., Tian, H., Liao, H., Pan, N., Pan, S., Ito, A., Jain, A. K., Kou-Giesbrecht, S., Joos, F., Sun, Q., Shi, H., Vuichard, N., Zhu, Q., Peng, C., Maggi, F., Tang, F. H. M., and Zaehle, S.: Global

- net climate effects of anthropogenic reactive nitrogen, Nature, https://doi.org/10.1038/s41586-024-07714-4, 2024.
- Henze, D. K., Hakami, A., and Seinfeld, J. H.: Development of the adjoint of GEOS-Chem, Atmos. Chem. Phys., 7, 2413–2433, https://doi.org/10.5194/acp-7-2413-2007, 2007.
- Hoesly, R. M., Smith, S. J., Feng, L., Klimont, Z., Janssens-Maenhout, G., Pitkanen, T., Seibert, J. J., Vu, L., Andres, R. J., Bolt, R. M., Bond, T. C., Dawidowski, L., Kholod, N., Kurokawa, J.-I., Li, M., Liu, L., Lu, Z., Moura, M. C. P., O'Rourke, P. R., and Zhang, Q.: Historical (1750–2014) anthropogenic emissions of reactive gases and aerosols from the Community Emissions Data System (CEDS), Geosci. Model Dev., 11, 369–408, https://doi.org/10.5194/gmd-11-369-2018, 2018.
- Huber, D. E., Steiner, A. L., and Kort, E. A.: Sensitivity of Modeled Soil NOx Emissions to Soil Moisture, Journal of Geophysical Research-Atmospheres, 128, https://doi.org/10.1029/2022jd037611, 2023.
- Hudman, R. C., Moore, N. E., Mebust, A. K., Martin, R. V., Russell, A. R., Valin, L. C., and Cohen, R. C.: Steps towards a mechanistic model of global soil nitric oxide emissions: implementation and space based-constraints, Atmos. Chem. Phys., 12, 7779–7795, https://doi.org/10.5194/acp-12-7779-2012, 2012.
- Hurtt, G. C., Chini, L., Sahajpal, R., Frolking, S., Bodirsky,
  B. L., Calvin, K., Doelman, J. C., Fisk, J., Fujimori, S.,
  Klein Goldewijk, K., Hasegawa, T., Havlik, P., Heinimann,
  A., Humpenöder, F., Jungclaus, J., Kaplan, J. O., Kennedy, J.,
  Krisztin, T., Lawrence, D., Lawrence, P., Ma, L., Mertz, O., Pongratz, J., Popp, A., Poulter, B., Riahi, K., Shevliakova, E., Stehfest, E., Thornton, P., Tubiello, F. N., van Vuuren, D. P., and
  Zhang, X.: Harmonization of global land use change and management for the period 850–2100 (LUH2) for CMIP6, Geosci.
  Model Dev., 13, 5425–5464, https://doi.org/10.5194/gmd-13-5425-2020, 2020.
- Hutchings, N., Webb, J., and Amon, B.: EMEP/EEA air pollutant emissions inventory guidebook 2023: 3.D Crop production and agricultural soils, European Environment Agency, https://www.eea.europa.eu/en/analysis/publications/emep-eea-guidebook-2023 (last access: 26 November 2025), 2023.
- Janssens-Maenhout, G., Crippa, M., Guizzardi, D., Muntean, M., Schaaf, E., Dentener, F., Bergamaschi, P., Pagliari, V., Olivier, J. G. J., Peters, J. A. H. W., van Aardenne, J. A., Monni, S., Doering, U., Petrescu, A. M. R., Solazzo, E., and Oreggioni, G. D.: EDGAR v4.3.2 Global Atlas of the three major greenhouse gas emissions for the period 1970–2012, Earth Syst. Sci. Data, 11, 959–1002, https://doi.org/10.5194/essd-11-959-2019, 2019.
- Jiang, Y., Deng, A. X., Bloszies, S., Huang, S., and Zhang, W. J.: Nonlinear response of soil ammonia emissions to fertilizer nitrogen, Biology and Fertility of Soils, 53, 269–274, https://doi.org/10.1007/s00374-017-1175-3, 2017.
- Jiang, Z., Zhu, R., Miyazaki, K., McDonald, B. C., Klimont, Z., Zheng, B., Boersma, K. F., Zhang, Q., Worden, H., Worden, J. R., Henze, D. K., Jones, D. B. A., van der Gon, H., and Eskes, H.: Decadal Variabilities in Tropospheric Nitrogen Oxides Over United States, Europe, and China, Journal of Geophysical Research-Atmospheres, 127, https://doi.org/10.1029/2021jd035872, 2022.
- Kou-Giesbrecht, S., Arora, V. K., Seiler, C., Arneth, A., Falk, S., Jain, A. K., Joos, F., Kennedy, D., Knauer, J., Sitch, S.,

- O'Sullivan, M., Pan, N., Sun, Q., Tian, H., Vuichard, N., and Zaehle, S.: Evaluating nitrogen cycling in terrestrial biosphere models: a disconnect between the carbon and nitrogen cycles, Earth Syst. Dynam., 14, 767–795, https://doi.org/10.5194/esd-14-767-2023, 2023.
- Lin, X. J., Ronald, V., de Laat, J., Huijnen, V., Mijling, B., Ding, J. Y., Eskes, H., Douros, J., Liu, M. Y., Zhang, X., and Liu, Z.: European Soil NOx Emissions Derived From Satellite NO2 Observations, Journal of Geophysical Research-Atmospheres, 129, https://doi.org/10.1029/2024jd041492, 2024.
- Liu, S. W., Lin, F., Wu, S., Ji, C., Sun, Y., Jin, Y. G., Li, S. Q., Li, Z. F., and Zou, J. W.: A meta-analysis of fertilizer-induced soil NO and combined NO+N2O emissions, Global Change Biology, 23, 2520–2532, https://doi.org/10.1111/gcb.13485, 2017.
- Lu, X., Ye, X. P., Zhou, M., Zhao, Y. H., Weng, H. J., Kong, H., Li, K., Gao, M., Zheng, B., Lin, J. T., Zhou, F., Zhang, Q., Wu, D. M., Zhang, L., and Zhang, Y. H.: The underappreciated role of agricultural soil nitrogen oxide emissions in ozone pollution regulation in North China, Nature Communications, 12, https://doi.org/10.1038/s41467-021-25147-9, 2021.
- Martin, R. V., Jacob, D. J., Chance, K., Kurosu, T. P., Palmer, P. I., and Evans, M. J.: Global inventory of nitrogen oxide emissions constrained by space-based observations of NO2-, Journal of Geophysical Research-Atmospheres, 108, 4537, https://doi.org/10.1029/2003jd003453, 2003.
- Matson, P. A., Naylor, R., and Ortiz-Monasterio, I.: Integration of environmental, agronomic, and economic aspects of fertilizer management, Science, 280, 112–115, https://doi.org/10.1126/science.280.5360.112, 1998.
- Park, R. J., Jacob, D. J., Field, B. D., Yantosca, R. M., and Chin, M.: Natural and transboundary pollution influences on sulfate-nitrate-ammonium aerosols in the United States: Implications for policy, Journal of Geophysical Research-Atmospheres, 109, https://doi.org/10.1029/2003jd004473, 2004.
- Peng, S. S., Lin, X., Thompson, R. L., Xi, Y., Liu, G., Hauglustaine, D., Lan, X., Poulter, B., Ramonet, M., Saunois, M., Yin, Y., Zhang, Z., Zheng, B., and Ciais, P.: Wetland emission and atmospheric sink changes explain methane growth in 2020, Nature, 612, 477, https://doi.org/10.1038/s41586-022-05447-w, 2022.
- Pinder, R. W., Davidson, E. A., Goodale, C. L., Greaver, T. L., Herrick, J. D., and Liu, L. L.: Climate change impacts of US reactive nitrogen, Proceedings of the National Academy of Sciences of the United States of America, 109, 7671–7675, https://doi.org/10.1073/pnas.1114243109, 2012.
- Rao, S., Klimont, Z., Smith, S. J., Van Dingenen, R., Dentener, F., Bouwman, L., Riahi, K., Amann, M., Bodirsky, B. L., van Vuuren, D. P., Reis, L. A., Calvin, K., Drouet, L., Fricko, O., Fujimori, S., Gernaat, D., Havlik, P., Harmsen, M., Hasegawa, T., Heyes, C., Hilaire, J., Luderer, G., Masui, T., Stehfest, E., Strefler, J., van der Sluis, S., and Tavoni, M.: Future air pollution in the Shared Socio-economic Pathways, Global Environmental Change-Human and Policy Dimensions, 42, 346–358, https://doi.org/10.1016/j.gloenvcha.2016.05.012, 2017.
- Rubin, H. J., Fu, J. S., Dentener, F., Li, R., Huang, K., and Fu, H.: Global nitrogen and sulfur deposition mapping using a measurement–model fusion approach, Atmos. Chem. Phys., 23, 7091–7102, https://doi.org/10.5194/acp-23-7091-2023, 2023.
- Russell, A. R., Perring, A. E., Valin, L. C., Bucsela, E. J., Browne, E. C., Wooldridge, P. J., and Cohen, R. C.: A high spa-

- tial resolution retrieval of NO<sub>2</sub> column densities from OMI: method and evaluation, Atmos. Chem. Phys., 11, 8543–8554, https://doi.org/10.5194/acp-11-8543-2011, 2011.
- Shcherbak, I., Millar, N., and Robertson, G. P.: Global metaanalysis of the nonlinear response of soil nitrous oxide (N2O) emissions to fertilizer nitrogen, Proceedings of the National Academy of Sciences of the United States of America, 111, 9199–9204, https://doi.org/10.1073/pnas.1322434111, 2014.
- Skiba, U., Medinets, S., Cardenas, L. M., Carnell, E. J., Hutchings, N., and Amon, B.: Assessing the contribution of soil NOx emissions to European atmospheric pollution, Environmental Research Letters, 16, https://doi.org/10.1088/1748-9326/abd2f2, 2021
- Stehfest, E. and Bouwman, L.: N2O and NO emission from agricultural fields and soils under natural vegetation: summarizing available measurement data and modeling of global annual emissions, Nutrient Cycling in Agroecosystems, 74, 207–228, https://doi.org/10.1007/s10705-006-9000-7, 2006.
- Steinkamp, J. and Lawrence, M. G.: Improvement and evaluation of simulated global biogenic soil NO emissions in an AC-GCM, Atmos. Chem. Phys., 11, 6063–6082, https://doi.org/10.5194/acp-11-6063-2011, 2011.
- Thornhill, G. D., Collins, W. J., Kramer, R. J., Olivié, D., Skeie, R. B., O'Connor, F. M., Abraham, N. L., Checa-Garcia, R., Bauer, S. E., Deushi, M., Emmons, L. K., Forster, P. M., Horowitz, L. W., Johnson, B., Keeble, J., Lamarque, J.-F., Michou, M., Mills, M. J., Mulcahy, J. P., Myhre, G., Nabat, P., Naik, V., Oshima, N., Schulz, M., Smith, C. J., Takemura, T., Tilmes, S., Wu, T., Zeng, G., and Zhang, J.: Effective radiative forcing from emissions of reactive gases and aerosols a multi-model comparison, Atmos. Chem. Phys., 21, 853–874, https://doi.org/10.5194/acp-21-853-2021, 2021.
- Tian, H., Pan, N., Thompson, R. L., Canadell, J. G., Suntharalingam, P., Regnier, P., Davidson, E. A., Prather, M., Ciais, P., Muntean, M., Pan, S., Winiwarter, W., Zaehle, S., Zhou, F., Jackson, R. B., Bange, H. W., Berthet, S., Bian, Z., Bianchi, D., Bouwman, A. F., Buitenhuis, E. T., Dutton, G., Hu, M., Ito, A., Jain, A. K., Jeltsch-Thömmes, A., Joos, F., Kou-Giesbrecht, S., Krummel, P. B., Lan, X., Landolfi, A., Lauerwald, R., Li, Y., Lu, C., Maavara, T., Manizza, M., Millet, D. B., Mühle, J., Patra, P. K., Peters, G. P., Qin, X., Raymond, P., Resplandy, L., Rosentreter, J. A., Shi, H., Sun, Q., Tonina, D., Tubiello, F. N., van der Werf, G. R., Vuichard, N., Wang, J., Wells, K. C., Western, L. M., Wilson, C., Yang, J., Yao, Y., You, Y., and Zhu, Q.: Global nitrous oxide budget (1980–2020), Earth Syst. Sci. Data, 16, 2543–2604, https://doi.org/10.5194/essd-16-2543-2024, 2024.
- Tian, H., Bian, Z., Shi, H., Qin, X., Pan, N., Lu, C., Pan, S., Tubiello, F. N., Chang, J., Conchedda, G., Liu, J., Mueller, N., Nishina, K., Xu, R., Yang, J., You, L., and Zhang, B.: History of anthropogenic Nitrogen inputs (HaNi) to the terrestrial biosphere: a 5 arcmin resolution annual dataset from 1860 to 2019, Earth Syst. Sci. Data, 14, 4551–4568, https://doi.org/10.5194/essd-14-4551-2022, 2022.
- Tian, H. Q., Yang, J., Xu, R. T., Lu, C. Q., Canadell, J. G., Davidson, E. A., Jackson, R. B., Arneth, A., Chang, J. F., Ciais, P., Gerber, S., Ito, A., Joos, F., Lienert, S., Messina, P., Olin, S., Pan, S. F., Peng, C. H., Saikawa, E., Thompson, R. L., Vuichard, N., Winiwarter, W., Zaehle, S., and Zhang, B. W.: Global soil nitrous oxide emissions since the preindustrial era estimated by

- an ensemble of terrestrial biosphere models: Magnitude, attribution, and uncertainty, Global Change Biology, 25, 640–659, https://doi.org/10.1111/gcb.14514, 2019.
- Wang, Y., Yao, Z. S., Zheng, X. H., Subramaniam, L., and Butterbach-Bahl, K.: A synthesis of nitric oxide emissions across global fertilized croplands from crop-specific emission factors, Global Change Biology, 28, 4395–4408, https://doi.org/10.1111/gcb.16193, 2022.
- Wang, Y., Ge, C., Garcia, L. C., Jenerette, G. D., Oikawa, P. Y., and Wang, J.: Improved modelling of soil NOx emissions in a high temperature agricultural region: role of background emissions on NO2 trend over the US, Environmental Research Letters, 16, https://doi.org/10.1088/1748-9326/ac16a3, 2021.
- Wang, Y., Yao, Z. S., Pan, Z. L., Guo, H. J., Chen, Y. C., Cai, Y. J., and Zheng, X. H.: Nonlinear response of soil nitric oxide emissions to fertilizer nitrogen across croplands, Biology and Fertility of Soils, 60, 483–492, https://doi.org/10.1007/s00374-024-01818-9, 2024.
- Weng, H. J., Lin, J. T., Martin, R., Millet, D. B., Jaegle, L., Ridley, D., Keller, C., Li, C., Du, M. X., and Meng, J.: Global high-resolution emissions of soil NOx, sea salt aerosols, and biogenic volatile organic compounds, Scientific Data, 7, https://doi.org/10.1038/s41597-020-0488-5, 2020.
- Yienger, J. J. and Levy, H.: Empirical-model of global soil-biogenic nox emissions, Journal of Geophysical Research-Atmospheres, 100, 11447–11464, https://doi.org/10.1029/95jd00370, 1995.
- Yuan, H., Dai, Y. J., Xiao, Z. Q., Ji, D. Y., and Shangguan, W.: Reprocessing the MODIS Leaf Area Index products for land surface and climate modelling, Remote Sensing of Environment, 115, 1171–1187, https://doi.org/10.1016/j.rse.2011.01.001, 2011.
- Zaehle, S. and Dalmonech, D.: Carbon-nitrogen interactions on land at global scales: current understanding in modelling climate biosphere feedbacks, Current Opinion in Environmental Sustainability, 3, 311–320, https://doi.org/10.1016/j.cosust.2011.08.008, 2011.
- Zaehle, S. and Friend, A. D.: Carbon and nitrogen cycle dynamics in the O-CN land surface model: 1. Model description, site-scale evaluation, and sensitivity to parameter estimates, Global Biogeochemical Cycles, 24, https://doi.org/10.1029/2009gb003521, 2010.
- Zhai, S. X., Jacob, D. J., Wang, X., Liu, Z. R., Wen, T. X., Shah, V., Li, K., Moch, J. M., Bates, K. H., Song, S. J., Shen, L., Zhang, Y. Z., Luo, G., Yu, F. Q., Sun, Y. L., Wang, L. T., Qi, M. Y., Tao, J., Gui, K., Xu, H. H., Zhang, Q., Zhao, T. L., Wang, Y. S., Lee, H. C., Choi, H., and Liao, H.: Control of particulate nitrate air pollution in China, Nature Geoscience, 14, 389, https://doi.org/10.1038/s41561-021-00726-z, 2021.
- Zhang, R. Y., Tie, X. X., and Bond, D. W.: Impacts of anthropogenic and natural NOx sources over the US on tropospheric chemistry, Proceedings of the National Academy of Sciences of the United States of America, 100, 1505–1509, https://doi.org/10.1073/pnas.252763799, 2003.
- Zhao, Y., Saunois, M., Bousquet, P., Lin, X., Hegglin, M. I., Canadell, J. G., Jackson, R. B., and Zheng, B.: Reconciling the bottom-up and top-down estimates of the methane chemical sink using multiple observations, Atmos. Chem. Phys., 23, 789–807, https://doi.org/10.5194/acp-23-789-2023, 2023.

Zhao, Y. H., Zheng, B., Saunois, M., Ciais, P., Hegglin, M. I., Lu, S. M., Li, Y. F., and Bousquet, P.: Air pollution modulates trends and variability of the global methane budget, Nature, 642, https://doi.org/10.1038/s41586-025-09004-z, 2025.